A receptor-inactivation model for single-celled habituation in *Stentor coeruleus*

Deepa Rajan and Wallace F. Marshall
Department of Biochemistry and Biophysics
University of California, San Francisco

Email: wallace.marshall@ucsf.edu

Abstract
The single-celled ciliate *Stentor* coeruleus demonstrates habituation to mechanical stimuli, showing that even single cells can manifest a basic form of learning. Although the ability of *Stentor* to habituate has been extensively documented, the mechanism of learning is currently not known. Here we take a bottom-up approach and investigate a simple biochemistry-based model based on prior electrophysiological measurements in *Stentor* along with general properties of receptor molecules. In this model, a mechanoreceptor senses the stimulus and leads to channel opening to change membrane potential, with a sufficient change in polarization triggering an action potential that drives contraction. Receptors that are activated can become tagged for inactivation, which may occur either via internalization, degradation, or some other mechanism. This activity-dependent inactivation provides a potential means for the cell to learn. Stochastic simulations of this model confirm that it is capable of showing habituation similar to what is seen in actual *Stentor* cells, including the lack of dishabituation and the apparently step-like response of individual cells during habituation. The model also can account for several observations that a previous two-state Markov model could not, namely, the dependence of habituation rate on stimulus magnitude, which had to be added onto the two state model but arises naturally in the receptor inactivation model; the rate of response recovery after cessation of stimulation; and the ability of high frequency stimulus sequences to drive faster habituation that results in a lower response probability. The model makes the prediction that application of high force stimuli that do not normally habituate should drive habituation to weaker stimuli due to decrease in the receptor number, which serves as an internal hidden variable. We confirm this prediction using two new sets of experiments involving alternation of weak and strong stimuli. The model is unable to account for the phenomenon of rate sensitivity, in which habituation caused by higher frequency stimuli is more easily reversed leading to a frequency dependence of response recovery. Such rate sensitivity has not been reported in *Stentor*. Here we carried out a new set of experiments which are consistent with the model's prediction of the lack of rate sensitivity. This work demonstrates how a simple model can suggest new ways to probe single-cell learning at an experimental level. Finally, we interpret the model in terms of a kernel estimator that the cell may use to guide its decisions about how to response to new stimuli as they arise based on information, or the lack thereof, from past stimuli.

Keywords
Basal learning; receptor degradation; receptor endocytosis; membrane potential; dishabituation; rate sensitivity; kernel estimator; frequency response; low-pass filter

Introduction

Cells are much more than just amorphous bags of enzymes, and their structural complexity is mirrored by a startling level of behavioral complexity that one would normally associate with animals that have a nervous system (Jennings 1906; Vertosick 2002; Bray 2011; Baluska and Levin 2016; Larson 2023). In addition to carrying out decision-making processes, cells are able to carry out at least simple forms of learning (Tang and Marshall 2018). One of the most fundamental forms of learning, habituation, is defined as the reduction in response to a stimulus following repeated application of that stimulus (Harris 1943; Thompson and Spencer 1966; Groves 1970; Rankin 2009). Habituation has been extensively documented in the giant single-celled organism *Stentor coeruleus* (Jennings 1902; Wood 1970a; Wood 1970b; Wood 1988a; Wood 1988b; Rajan 2023). *Stentor* is a giant ciliate known for its amazing powers of regeneration (Tartar 1961; Marshall 2021). When undisturbed, the cell stretches out into a cone-like shape, attaching to pond plants via a holdfast and feeding by means of a membranellar band of cilia at its anterior end (**Figure 1A**). When disturbed by a mechanical stimulus, the cell contracts downwards towards its point of attachment (Jones 1970; Newman 1972), by means of a series of parallel myonemes that run the length of the cell. These myonemes are composed of calcium binding EF hand proteins in the centrin family (Huang and Pitelka, 1973; Maloney 2005). The large size of *Stentor* cells, and the extensive shape change that occurs during contraction, makes the contraction response easy to observe and quantify (**Figure 1B**). When *Stentor* cells are exposed to a repeated stimulus, they will gradually stop responding to it, a response that shows many of the features that characterize habituation in other organisms (Wood 1970).

Compared to other cell types, *Stentor* is a convenient model system in which to study habituation at the single-cell level due to the ease with which the behavior (contraction) can be observed; the unambiguous nature of the essentially binary contraction response, which makes it easy to classify cells into contracted or non-contracted states with minimal uncertainty; the ability to monitor contraction and habituation in many cells at the same time in a single dish, which allows statistical numbers to be rapidly collected; and the short timescale necessary to observe habituation (20-30 min)., which allows experiments to be replicated with ease. The genome of *Stentor* has been sequenced (Slabodnick 2017) and RNAi methods are available to perturb gene expression (Slabodnick 2014). The molecular components of the *Stentor* cell have been cataloged by means of proteomics (Lin 2022) and transcriptomics (Sood 2022), all of which make it an excellent model system for exploring the mechanism of single-celled learning.

We confirmed the ability of *Stentor* cells to habituate, using a computer-controlled device to provide mechanical stimuli to *Stentor* cells (Rajan 2023a). Our results matched the results of Wood in that weaker stimuli led to faster and more extensive loss of the contraction response (**Figure 1C**). Unlike the work of Wood (1970a), in our experiments we tracked the responses of individual cells, and found that while a population of cells showed the gradual reduction in response probability that Wood had reported, when individual cells were observed, they appeared to undergo a switch-like response from a highly responsive to a less responsive state (**Figure 1D**). By using model-fitting procedures including hidden Markov model reconstruction, we found that a two-state model (**Figure 1E**) could account for the observed behavior, but only if the reverse transition probability, from the non-response back to the responsive state, was extremely slow.

Our previous study showed that a two-state model is sufficient to account for the learning behavior of single cells receiving stimuli at a constant frequency. This model can correct match the dynamics of habituation in populations of cells, the step-like response observed from individual cells, and allowed the effect of force on habituation rate to be represented as an input that varies one of the transition rates. It is worth noting that this last point, the ability to account for the force dependence of habituation rate, was something that had to be directly built into the model parameters by allowing one rate (the forward transition rate p12 from the responsive to the non-responsive state) to vary as a function of the force. This was not a prediction that followed automatically from any underlying model, just an assumption that needed to be added to allow the model to fit habituation data at both force levels. The force dependence of habituation was therefore something that the two-state model could accommodate, but only by adding an addition assumption.

Further experiments showed that the two-state model with force-dependent forward transition is NOT sufficient to represent the response of cells to different stimulus periods, nor could it represent the response recovery after cessation of the stimulus. With respect to different stimulus periods, it was found that when stimuli were applied at a very high frequency (1 per 1.2 seconds rather than 1 per minute), the habituation rate was higher when expressed in terms of time, but lower when expressed in terms of stimulus number. This is not consistent with a two-state model that has the chance to switch states with each stimulus, and suggested that the system was responding not just to the stimulus sequence as a discrete sequence of inputs, but also to the timing with which they were received.

With respect to response recovery, it is known that once the habituating stimulus ceases, *Stentor* cells will gradually return to the original pre-habituation response probability over a timescale of tens of minutes hours (Wood 1970a). In the two-state model, response recovery is driven by the reverse transition (probability p21 in **Figure 1E**) from non-responsive back to responsive state. When this parameter was adjusted to allow a good fit of single cell habituation data, the best fit value was extremely low (0.001 min^{-1}) which was consistent with the fact that virtually all cells were observed to undergo a single transition to the non-responsive state, and never back to the responsive state. But using such a low value of the reverse transition probability means that the response recovery should take place on a time scale of 5 hours, rather than the 20 minute halftime observed in the same experimental measurements used to fit the transition rates (Rajan 2023a). This disparity between the reverse transition rate needed to explain the habituation curves during learning, with the transition rate needed to explain the response recovery during forgetting, was apparently a serious flaw in terms of the model's ability to account for experimental data.

Thus, the two-state model has (at least) three major shortcoming when faced with actual data: (1) it does not predict force dependence, but instead requires this to be added as an assumption; (2) it does not predict the dependence of habituation rate on stimulus frequency; and (3) it does not predict a realistic response recovery rate when its parameters are chosen so as to represent single-cell habituation dynamics.

Another issue with the two-state model is implementation - although a model with two states is in some sense the simplest possible model, this view of simplicity comes more from the perspective of theoretical computer science, in which the finite state machine forms the lowest rung of a hierarchy of increasingly complex computational models, and the two-state

model is the simplest non-trivial finite state machine. While we believe that there may be many contexts in which such a theoretical computer science perspective is appropriate (Condon 2018), there is always the question of how to generate such states at a molecular level. In fact, implementing a two-state with molecules is non-trivial. Certainly, there are a large number of examples in which a single molecule can switch between two distinct functional states, and such molecules play important roles in a huge number of biological processes (Philips 2020). But for a molecular switch to create a two-state system at the level of a whole cell would require a way to coordinate the activity of many molecules so that they all switch into one state or another, and it is not obvious a priori how to do this. Thus, a two-state switch-like behavior at the level of an entire cell may not actually be that simple to implement.

From a molecular perspective, a much simpler model would actually be one in which a population of molecules switch state independently, leading to a continuous rather than switch-like response. For example, we can envision a mechanism in which the mechanoreceptor itself, or some downstream molecule involved in signal transduction, is degraded or inactivated with a probability that depends on the current stimulus level, such that continued stimulation would lead to a gradual loss of receptor function. Here we investigate such a model in which we represent the inactivation or degradation of a molecule involved in mechanical force transduction, coupled with a thresholding mechanism based on previously published electrophysiology studies (Wood 1970b; Wood 1988a; Wood 1988b), and show that indeed such a mechanism can produce a switch-like behavioral transition in the cells even though the underlying "learning" process is based on a continuous variable representing the quantity of functional receptor. In this sense it is just as good as the two-state Markov model. Unlike the two-state model, the receptor inactivation model directly predicts, without any additional assumptions and using a single parameter set, the dependence of habituation rate on force, the effects of increased stimulus frequency, and the timescale of response recovery. We further test this model using new experiments specifically designed to test model predictions, including an evaluation of “rate sensitivity” in terms of a dependence of response recovery rate on stimulus frequency. Unlike many other habituating organisms, *Stentor coeruleus,* under the conditions we tested, does not appear to display rate sensitivity. Based on these results, we suggest that the receptor inactivation model, while still highly simplistic, is both more biologically motivated and also more effective, as a model, compared to our previous two-state model.

Results

Habituation and response recovery in a receptor-inactivation model

As a first step towards modeling possible pathways that might produce habituation, we started with a highly simplified scenario (**Figure 2A**) in which a mechanoreceptor linked to an ion channel responds to mechanical stimulation to open a channel and allow ions to flow across the membrane, thereby changing membrane potential. If the membrane potential crosses a threshold, calcium channels open allowing calcium to enter the cell. It is known that the contraction of *Stentor* is driven by myonemes composed of calcium-binding EF hand proteins (Huang and Pitelka 1973; Maloney 2005). For the purposes of this model, we assume that the calcium channel opening is an all or nothing response, such that whenever the membrane potential crosses a threshold, a contraction response is recorded. This assumption is consistent with prior demonstrations of a classical action potential in *Stentor* (Wood 1970b). Many receptors undergo inactivation and degradation following activation, in some cases via endocytic internalization and in other cases by proteolytic degradation (Kholodenko 2003, Shankaran 2007, Lin and Man 2013, Rosendale 2017). A wide variety of receptors and channels are known to be able to mediate mechanosensation in different organisms and tissues, including NOMPC/TRP channels, DEG/ENaC channels, and Piezo channels (reviewed in Katta 2015). We do not know the molecular identify of the *Stentor* mechanoreceptor, but among the various classes of mechanoreceptors in other species, many are part of receptor and channel families known to undergo internalization, ubiquitination, and/or degradation following activation (reviewed in Estadella 2020).

To represent receptor inactivation/degradation, we allow each receptor molecule to exist in a marked or unmarked state. When a receptor is activated, it becomes marked with a certain probability. Such marked receptors then undergo degradation at a specified rate. Both marked and unmarked receptors also undergo basal degradation at the same rate, lower than the activation-mediated degradation rate, and the total receptor number increases over time due to receptor synthesis, which is assumed to occur at a constant rate. Details of the model, including the model parameters that describe receptor protein dynamics, input-output function for receptor activation, and electrical coupling, are given in Methods.

Simulations of this model using parameters obtained from a parameter search process show that indeed habituation can be accounted for by this simple mechanism (**Figure 2B**). As plotted in the graph, during continuous stimulation, the number of receptors (blue) gradually decreases, leading to a correlated decrease in response probability (red). During habituation, the number of receptors marked for degradation rises and then reaches a plateau at steady state. After the stimulus ceases (after 30 stimuli), the response probability gradually returns back to its initial value, driven by the synthesis of new receptors to replace those that had been lost by degradation. The parameter choice used in this simulation yielded an initial response probability, habituated response probability, habituation timescale, and timescale of response recovery (forgetting) that were all comparable to what had previously been observed experimentally (Wood 1970a; Rajan 2023).

The ability to account for the response recovery timescale is notable. One major difficulty with the two-state model that we previously proposed is its inability to fit both the habituation rate as well as the response recovery rate that are seen in actual *Stentor* cells (Rajan 2023). The reason is that in order to account for the switch-like behavior seen in single *Stentor* cells, it is

necessary for the reverse transition rate (from non-response to response) in the two-state model to be extremely small. But this same rate constant is what determines the response recovery after cessation of stimuli in that model. In contrast, the receptor-inactivation model accommodates the observed time-scale of response recovery after stimuli are stopped (see **Figure 2B** timepoints 31-60).

One unusual feature of habituation in *Stentor*, that is distinct from habituation in most animal species, is the lack of dishabituation, i.e. the ability of a single strong stimulus, when applied to a habituated organism, to restore responsiveness to weaker stimuli to which it had become habituated. This is a common feature in many cases of habituation (Thompson and Spencer 1966), but experiments by Wood have shown that it does not occur in *Stentor coeruleus* (Wood 1970a). In the receptor inactivation model, there is no mechanism for the stimulus to relieve the habituated state. If anything, applying a strong stimulus, which tends to mark and inactivate more receptors, would only lead to stronger habituation. Simulations of the model confirm this intuition. As seen in **Figure 2C**, when a single strong stimulus is applied after a series of low for habituating pulses, it drives a contractile response because the stimulus is strong enough to activate a large enough number of receptors to cross the activation threshold, but after that pulse when the stimulus returns to the previous lower magnitude, the response drops back down to what it would have been if the strong stimulus were never applied. Thus, our model is in agreement with the known lack of dishabituation in *Stentor*.

Receptor inactivation model recapitulates step-like habituation response of individual cells

One of the main experimental facts that led to the two-state model was the observation that even though a population of cells shows a graded response, individual cells showed a step-like response, apparently switching from one state in which the response probability was high, to a new state in which the response probability was low. The receptor inactivation model might seem inconsistent with this observation, since it is based on a graded internal variable in the form of the total receptor number. But it is important to note that this graded internal variable is then read out by a non-linear process involving a thresholding operation. As the graded variable drops below a threshold, a sudden drop in response may be observed. To test this idea, we carried out a stochastic simulation of the receptor inactivation model (see Methods). As shown in **Figure 2D**, this model incorporates fluctuations in the rate of receptor degradation and synthesis, and can simulate the response of individual cells as shown by the spiking response indicated by the purple bars. It can be seen in the example shown in **Figure 2D** that a cell that initially contracts on every stimulus appears to switch to a lower frequency of response. When this simulation is repeated many times, the average response of the simulations recapitulates the graded response of the population (**Figure 2E**). We previously described a statistical test for stepping (Rajan 2023a) based on the use of Fisher's exact test to first infer the most likely time point at which a step might occur and then test the null hypothesis that the frequency of response is the same before and after the inferred step. Low P-values in this test indicate that the frequencies are unlikely to be the same and thus that a step has occurred. We previously applied this test to experimental data on *Stentor* habituation and found that there was strong statistical support for most cells taking a single step but not two or more steps (Rajan 2023b). Stochastic stimulations of the receptor inactivation model

also indicate that a large fraction of cells are taking a single step based on the same statistical test (**Figure 2F**). Thus, the biochemical receptor inactivation model seems capable of accounting for the apparent step-like response during *Stentor* habituation.

Receptor inactivation model recapitulates dependence on magnitude of stimulus

One highly conserved aspect of habituation that is also seen in *Stentor* is the fact that habituation takes place more rapidly and more extensively in response to low force stimuli compared to higher force stimuli, such that with sufficiently strong stimuli, habituation barely takes place at all on the timescale of an hour. In our previous two-state model, this force-dependent difference in habituation rates had to be accommodated by assuming that one or more parameters in the two-state model were inherently force-sensitive. Parameter fitting suggested that the main parameter affected by the force level was the forward transition rate (from the responsive to the non-responsive state).

When we simulated the receptor-inactivation model, we found that in fact a single set of parameters could account for the habituation dynamics of two different force levels, such that low force stimuli caused extensive habituation (**Figure 3A**) while high force stimuli caused little habituation (**Figure 3B**), a trend that extended over a wide range of stimulus magnitudes (**Figure 3C**), thus recapitulating what has been seen in experiments without the need to arbitrarily retune parameters to model different levels of force as we had previously done for the two-state model (Rajan 2023). Thus, the receptor inactivation model can explain this phenomenon in a more parsimonious way compared to our previous two-state model.

Dependence of habituation on frequency of stimulation

As discussed above, we previously showed experimentally (Rajan 2023) that stimuli applied at a higher frequency (1 per second versus 1 per minute) led to faster habituation in terms of the actual time, but slower habituation in terms of the number of stimuli - that is, habituation to the same extent required a larger number of stimuli at high frequency, but because the time between stimuli was so low, the overall time for habituation was less than seen with lower frequency stimulation. This phenomenon was not explainable in terms of the two-state model. In contrast, as shown in **Figure 3D**, our simulation predicts faster habituation for stimuli applied at lower frequencies (compare to **Figure 3A** which uses the same force magnitude but lower frequency).

Wood (1970a) reported that compared to the standard stimulus period of 1 per minute, stimuli of lower frequency produced less of a decrease in response probability at steady state. Our simulation results recapitulate this result (**Figure 3E**). Conversely, we also found that higher frequency stimulation could produce more extensive habitation in the sense that the response probability at steady state was lower than with low frequency stimulation.

Taken together, our simulations indicates that the highly simplistic biochemical model for habituation based on receptor inactivation can account for all of the previously reported phenomenological features of habituation in *Stentor*, namely: the habituation response for a population of cells, the apparently step-like response of individual cells, faster habituation in response to weaker stimuli, the consistent time-scales of both habituation and response

recovery, and the dependence of habituation extent on stimulus frequency. Many of these features could not be accounted for by the previous two-state model. In light of the apparently reasonable predictions of the biochemical model, we next used the model to make new predictions which we then test with customized experiments.

Experimental test of model prediction: high force stimuli followed by low force stimulus

A comparison of **Figure 3A** and **Figure 3B** show an interesting feature, that although the cell fails to habituate significantly to a high force stimulus, the total receptor number still decreases during high force stimulation. The reason that habituation is not observed in this model is that even when the receptor number drops substantially, if the stimulus is strong enough, the remaining receptors become fully activated and keep the system above the threshold for triggering an action potential. The fact that receptor number drops during exposure to high force stimuli that do not yield observable habituation leads to a prediction: if we were to follow a series of high force stimuli with a low force stimulus, the cell should show a reduced response to that low force stimulus compared to if it were applied to a naive cell. **Figure 4A** illustrates the experiment, and **Figure 4B** shows the result of simulation. It can be seen that the model predicts a reduced response to the first low-force stimulus following the high force stimuli.

To test this prediction, we used our stepper motor-based habituation device (Rajan 2023b) to stimulate cells with a high force stimulus for 19 iterations, followed by 41 low force stimuli. The results are plotted in **Figure 4C**. Also plotted, for comparison is the result of a comparable experiment but using only low force stimuli. It can be seen that despite little reduction in response during the high force stimulus, the response to the subsequent low force stimulus is indeed reduced, to a level comparable to what would have been observed if low force stimulation had been used throughout the experiment. A similar effect was seen using an even higher force for the initial training. This experimental result confirms the prediction of our receptor degradation model. This result is fundamentally incompatible with our previous two-state model, in which the low transition probability to the non-responsive state during high frequency stimulation would mean that when the low frequency stimuli were applied, the response rate would still be high initially, and only start to decrease as successive low force stimuli were applied.

Experimental test of model prediction: interleaved high and low force stimuli

The previous simulation and experimental comparison supports the idea that there is a hidden variable, which in the model represents the quantity of receptors, which can change even response to stimuli that have little observable effect on habituation. As an alternative way to compare the model with predictions, we simulated an experiment in which strong and weak stimuli were alternatively applied in an interleaved fashion. As shown in **Figure 4D**, simulations of such an interleaved weak/strong stimulus experiment predict that the response probability to the low magnitude stimulus should still show habituation but this will not carry over to the strong force stimulus. We note that this prediction is entirely different from the prediction made by the two-state model, in which once a cell is in the non-responsive state, it

would not respond to either stimulus, thus the low magnitude stimuli would tend to drive faster habituation of the higher magnitude stimuli. We thus have a clear distinct set of predictions for the two models - the receptor inactivation model predicts that interleaved stimuli would show habituation of the responses to the low force stimuli, but not to the high force stimuli, whereas the two-state model predicts that interleaved stimuli would lead to faster habituation of the high force stimuli than would be seen if the high force stimuli were presented exclusively.

We tested the predictions of the two models experimentally in *Stentor* cells, by using our stepper motor habituation device to provide alternating low and high force taps. As shown in **Figure 4E**, the results match the prediction of the receptor-inactivation model, in that the response probability to the low magnitude stimuli showed a continuous decrease, while the response to the high magnitude stimuli continued to stay high comparable to what has been seen in high force only experiments.

Experimental test of model prediction: apparent lack of rate sensitivity on response recovery time

One commonly observed feature of habituation in animals is "rate sensitivity" which is defined as faster recovery of response following cessation of stimulus when the stimulus frequency was higher (Staddon 1993; Staddon and Higa 1996). Previous studies investigating the effect of stimulus frequency on habituation in *Stentor* (Wood 1970a; Rajan 2023a) reported effects on the rate and extent of habituation but did not address whether or not rate sensitivity occurs in this system.

Using our simulation of the receptor inactivation model, we calculated the predicted response recovery time as a function of the stimulus frequency. **Figure 5A,B, C** depict simulation results using the same parameter values and the same stimulus magnitude, but with progressively increasing stimulus frequencies. **Figure 5D** summarizes the response recovery half-times calculated for a range of stimulus frequencies. In contrast to **Figure 3E** which showed that the habituation extent depends on stimulus frequency, our model indicates that the response recovery time is changes very little as a function of stimulus frequency, with a slight increase in recovery time for very high frequencies. The reason for this increase can be seen from the simulation results in panels A-C, where the higher frequency stimulation leads to a more extensive drop in the receptor number, with a correspondingly greater drop in the response probability. Because higher frequency stimulation causes greater inactivation of receptors in a given length of time, it takes longer to recover full response after the stimulation ceases. We note that this type of dependence, in which the response recovery time is greater for higher stimuli, is the opposite of what has been reported for "rate sensitivity" in animal habituation. We conclude that the receptor inactivation model described here cannot account for the rate-sensitivity phenomena seen in other organisms.

We therefore asked whether the habituation of *Stentor* cells actually exhibits rate sensitivity, by habituating cells with the same force stimulus at two different frequencies: 1 tap per 1.2 sec versus 1 tap per minute. As shown in **Figure 6E**, the response recovery took place with virtually indistinguishable kinetics in both cases, with, if anything, a slight lag in recovery for cells habituated with a higher frequency stimulus. These results suggest that *Stentor* may

not display rate sensitivity, at least not under the parameters of our current experimental conditions, which would be consistent with the prediction of the receptor inactivation model.

Discussion

Evaluation of biochemical model with respect to empirical data about Stentor habituation

Habituation is defined as a decrement in response probability following repeated exposure to a constant stimulus (Harris 1943). However, over the years experimental psychology studies in various animals from invertebrates to humans have revealed a number of additional features that often accompany habituation. Thompson and Spencer (1966) in a comprehensive review of habituation in multiple animal model systems, defined nine widespread features that habituation displays. This list was updated in a more recent publication (Rankin 2009) which clarified the wording and concepts and added one more. Here we consider these nine, as well as a tenth feature that has been noted by others, and discuss the extent to which these features are reflected in our model or in experimental studies of *Stentor* habituation.

1. *Repeated application of a stimulus results in decreased response, usually as a decaying exponential function of the number of stimulus presentations.*

As shown in **Figure 2B**, our model shows the decrease in response, and the form is visually similar to an exponential, as explained by the fact that the mechanism for the response decrement is the first-order decay of the marked receptors. Prior studies in *Stentor* also show such a decay curve during habituation (Rajan 2023a). So in this case, the model agrees with experiment, both of which agree with the summary of Thompson and Spencer.

2. After the stimulus stops, the response recovers over time (forgetting).

As shown in **Figure 2B**, when the stimulus ceases, the response recovers over time. Response recovery over a similar timescale has been documented in *Stentor* (Wood 1970a; Rajan 2023a). So again, in this case, the model agrees with experiment, both of which agree with the summary of Thompson and Spencer.

3. As cycles of habituation and recovery are repeated, successive rounds of habituation take place more rapidly (potentiation).

Our model cannot produce this effect, because once the number of receptors has returned to its initial value, the system is identical to its state at the start of the whole experiment, and so the subsequent behavior will also need to be the same. This will be the case no matter how parameter values are chosen. This is a clear difference with the summary of Thompson and Spencer. Wood (1970) reported that after one round of habituation followed by a 6 hour rest period, when a second round of habituation was carried out, the habituation reached its minimum value in 40 minutes rather than 45 minutes for the first round, a different in habituation rate which was statistically significant. The difference was small, but in any case our model would predict no difference whatsoever, provided the response had fully recovered during the rest period. This, therefore, may be one aspect of habituation in *Stentor* that the model cannot predict. Potentiation of this type would apparently require that some molecular change persists on a time scale that is longer than the over recovery of the response, suggesting the presence of an additional molecular component besides the receptor.

4. Higher frequency of stimulation leads to faster and/or more extensive reduction in response, and more rapid response recovery after the stimulus ceases.

Our model recapitulates the first part of this effect (**Figure 3E**), which has also been experimentally demonstrated in *Stentor* (Wood 1970a; Rajan 2023). So in this case, the model agrees with experiment, both of which agree with the summary of Thompson and Spencer.

The second part of this feature, the increased rate of recovery when habituation is performed with higher frequency stimuli ("rate sensitivity") was not included in Thompson and Spencer's list of nine characteristic features of habituation, but was added in their 2008 revision (Rankin 2008). Rate sensitivity has been observed in rats (Davis 1970), *Aplysia* (Byrne 1982), and *C. elegans* (Rankin and Broster 1992), but was not reported in Wood's analysis of habituation in *Stentor* (1970). Our model does not show such behavior. On the contrary, the model predicts that higher frequency stimuli might lead to slightly slower, rather than faster, response recovery (**Figure 5D**). Our experiments presented here also failed to detect evidence for rate sensitivity in *Stentor* under the particular conditions we employed (**Figure 5E**), so in this case the model agrees with experiments in *Stentor*, but both disagree with reports on habituation in animals.

5. Weaker stimuli produce faster or more extensive habituation compared to strong stimuli which, in some cases, may not yield habituation at all.

Our model recapitulates this effect (**Figure 3C**), which has also been experimentally demonstrated in *Stentor* (Wood 1970a; Rajan 2023). So in this case, the model agrees with experiment, both of which agree with the summary of Thompson and Spencer.

6. Prolonged exposure to a stimulus after the point at which response has ceased leads to a slower response recovery.

Our initial investigation of this phenomenon within our modeling framework does not show such an effect. However, we have not systematically explored all possible parameter values. This effect could in principle be produced if the response probability was a sufficiently sharp nonlinear function of receptor number, such that response could be extinguished before the receptor number drops to zero, in which case further exposure to the stimulus would further deplete the receptor, thus requiring a longer time to recover the response. But this effect is not seen with our current parameter set, and it remains an open question whether *Stentor* even displays such a phenomenon.

7. Habituation to a given stimulus exhibits stimulus confers reduced response to other stimuli.

Our model would not produce this effect given that the receptor that undergoes inactivation/degradation is presumably specific to the mechanical stimulus. Wood (1970a) has shown that the response to electrical pulses is not altered by habituation to mechanical stimulation, so in this case our model agrees with experiment.

8. Presentation of a strong stimulus can lead to recovery of response (dishabituation).

Lack of dishabituation in *Stentor* has been demonstrated (Wood 1970a). Our model also does not display dishabituation (**Figure 2D**), so in this case the model agrees with experiments in *Stentor*, but neither agrees with the trend reported by Thompson and Spencer.

9. When a strong stimulus that produces dishabituation is applied repeatedly, its effect diminishes.

Because *Stentor* cells do not dishabituate, this feature is not applicable.

10. Some experimental protocols may produce habituation that persists for hours, days, or weeks (long term habituation).

In our model, the response recovery time is only a function of how small the number of receptors was at the end of the stimulus sequence, and the rate of receptor synthesis. There is no way to manipulate the stimulus sequence protocol to slow down the response recovery, other than driving the receptor number as low as possible. We therefore do not expect that the model as formulated could account for long term habituation. Long term habituation was not reported by Wood (1970a). This is thus a case where the model agrees with experiments, but neither agrees with the reported feature, but in this case this lack of agreement does not seem significant given that this type of behavior is apparently only seen in a few special cases (Rankin 2008).

Limitations and future directions for experimental tests of model predictions

Although we report here a lack of evidence for rate sensitivity in *Stentor*, we acknowledge the very real possibility that rate sensitivity might be a component of *Stentor* habituation under alternative experimental conditions and training regimes. Cells that undergo training for 12 hours at a frequency of 1 stimulus per minute (low-frequency) do not habituate as completely as cells that experience the same length of training at frequency of 1 stimulus per 1.2 seconds (high-frequency), such that the fraction of *Stentor* contracted at time zero post-training is slightly lower for the latter group (**Figure 5E**). Given that claims of rate sensitivity in other organisms are typically made when habituation has reached the same steady state level in both high-frequency and low-frequency training groups, this slight difference in contraction fractions at the conclusion of *Stentor* training may be a possible confounder. Furthermore, the cells used for the low-frequency training group were sourced from a highly dense culture that was over 5 weeks old, which is older than the culture state when the cells were isolated for the high-frequency experiments. The difference in culture age or cell density may have some effect on habituation, although this has not been previously reported. These considerations suggest that in the future, habituation experiments should be carried out under maximally consistent cell culture conditions. It will also be useful to explore different training lengths to determine if rate sensitivity emerges in *Stentor* at longer timescales.

Hidden variables and temporal response

A major difference between the present model and our previous two-state model is that in the previous model, the states were directly observable based on the frequency of response. In the present model, there are two hidden variables, meaning that they cannot be directly observed in our habituation experiments: the total number of receptors, and the number of marked receptors targeted for degradation. Both of these can potentially influence the dynamics of observed behaviors. The fact that receptor number can decrease during high force stimulation explains the experimental results of **Figure 4C** and **4E**. It is important to note that

the current model is extremely simplified, and that if more detail were to be added, such as representing separate variables for ubiquitinated receptors and internalized receptors, the additional hidden variables could support even richer sets of behaviors. The goal of the present study was to determine how many features of *Stentor* habituation could be accounted for with the simplest possible model, as a guide for future experiments and further model development.

Molecular implementations of the receptor inactivation model

Our model is based on the assumption that the mechanoreceptor that receives the mechanical stimulus, or some element downstream of the receptor, can, when activated, be subsequently inactivated. Such inactivation could in principle occur by a variety of mechanisms including proteolytic degradation, endocytic internalization, or post-translational modifications such as phosphorylation. Determining which of these types of inactivation may be at play during habituation in *Stentor* is an interesting challenge for future work, and we propose two broad types of strategies for pursuing this question. One approach would be an unbiased method in which various "omics" methods, like proteomics and phosphoproteomics, could be brought to bear to identify molecular changes that take place as the cell becomes habituated. Based on our model, relevant modifications would be those for which the time scale at which the modification occurs matches the time scale of habituation, and for which the time scale at which the modification reverts back to baseline matches the time scale of forgetting. Such an approach could be successful if the inactivating modification is something that can be detected by appropriate omics methods. But some forms of inactivation, such as internalization into the cell interior to remove the receptor from the plasma membrane, would not be revealed by standard proteomic analyses of whole cells. The alternative approach would to be guess the identity of the receptor, and then directly test whether it is subject to any identifiable modifications that might lead to its inactivation or degradation. At present, this approach seems less promising since it is not obvious what protein plays the role of the mechanoreceptor. In any case we believe that this is an area that is ripe for experimental investigation using the tools of molecular cell biology.

We also note that there may be other *Stentor* behaviors that might employ a similar mechanism for decision making. The related *Stentor* species *Stentor roeseli* has multiple possible evasion mechanisms beyond just contraction, including bending and ciliary reversal, and appears to try them out in a pre-defined sequence (Jennings 1902; Jennings 1906; Dexter 2019; Trinh 2019). If the different possible responses are triggered by a single underlying receptor molecule as it passes distinct thresholds, this could potentially explain their sequential deployment in a predictable order. Such a model would make two predictions. First, the time spent in the earlier behaviors (bending, reversal) should decrease over time such that the cell will move more rapidly to the later behaviors (contraction, detachment). This effect was reported by Jennings (1902; 1906), and while not explicitly reported in Dexter (2019), this trend is clearly seen in their data (Marshall 2019). Second, if a single underlying molecule such as the receptor for the noxious stimulus is being inactivated/degraded over time during the procedure, then when the stimulus is removed, the receptor would be re-synthesized such that if a stimulus were to be re-applied at various time-points during the re-synthesis period, the

evasion behaviors would be expected to be deployed in the opposite order from when the cell was initially trained. To our knowledge, this experiment has not been done.

What do cells learn? A kernel estimation framework for Stentor habituation

We have previously tended to consider the habituation process as one in which the cell learns something about the stimulus - deciding if it is caused by a threatening or non-threatening condition in its environment. For *Stentor*, the cell needs to make a quick decision, when it comes into contact with a moving object, whether or not to trigger its contraction response. Contraction is rapid and effective, but energetically costly. The contraction process itself does not use ATP, just calcium binding to centrin family proteins (Huang and Pitelka 1973; Maloney 2005) but afterwards, it is necessary to pump all that calcium back out, and that incurs a huge energetic cost. Certainly, if a cell is struck with a very strong force that might be typical of a larger predator, contracting would be a good decision. For a sufficiently strong force, it might always make sense to contract since even though this burns energy, at least the cell is not consumed by a predator. A weaker force might be less obviously threatening, but it could still be generated by a large and threatening predator, if the initial contact was not head-on. The only way to know if a weak stimulus is "typical" would be if multiple such stimuli had been received. Therefore, a good strategy would be to stop contracting if weak stimuli were being detected at some baseline rate, but if a long period goes by without any stimuli, even weak ones, it could be an effective strategy to initially contract when the next stimulus arrives, even if weak, until enough stimuli have been received to make a determination about how typical the weak stimulus is. In this view, the cell is carrying out an estimation process using impulse data that arrives at random times. A classical way to handle such an estimation problem is with kernel estimators, where each impulse is convolved with some impulse response that extends over time, allowing inputs to be integrated over some window, with gradually reducing influence from inputs that recede into the past. In our model, each stimulus drives the marking of some set of receptors, which then gradually inactivate over time. In this case the kernel is an exponentially decaying function set by the destruction rate of marked receptors. Integration is carried out by the combined effect of all receptor-linked channels on membrane potential.

A recent theoretical study has shown how habituation in general may be cast in the framework of linear filters (Gershman 2024). In our model, each stimulus causes a set of receptors to be marked, and those marked receptors then undergo exponential decay. This exponential decay is literally the impulse response of a first order IIR filter. Furthermore, our simulations of habituation extent versus stimulus frequency (**Figure 3E**) shows that the cell is acting like a low-pass filter, transmitting a pulse train of input stimuli into a pulse train of output stimuli with a gain that decreases as frequency increases. A Bode plot indicates a corner frequency of approximately 2 min^{-1} and an approximately 20dB per decade roll off characteristic of a single-pole filter (**Supplemental Figure S1**). It would be potentially interesting to explore how the parameters of the current bottom-up molecular model may relate to the statistical framework of Gershman's linear filter model, using this first order low-pass filter property to translate between the two model frameworks.

There has been a long discussion in psychology and in philosophy of mind about the definition of learning. Our model represents an example in which the term "learning" is best

construed as indicating a process in which an organism updates the parameters of an internal model of the world. Here, the number of receptors serves as a proxy for how safe the environment is, with high numbers of receptors indicating that either there is a definitive threat nearby, or else there is not enough information to know if there is a threat. Often when discussing habituation in a single-cell context, there is a debate about whether habituation is really "just" adaptation. In a multicellular organism, the distinction is based on where the habituation occurs - if it occurs at the sensory or motor levels, it is called adaptation, whereas if it occurs central, i.e. within the nervous system, it is called habituation (Staddon and Higa 1996; Kuenen 1981, Torre 1995). The distinction thus has nothing to do with what the process is, or how it is implemented, but rather with how it is used by the organism. In the case of *Stentor*, given that the receptor number is reflecting information about the world, on the basis of which the cell can make a decision about future responses, it does seem that habituation is indeed the more apt description.

Methods

Mathematical model for habituation based on mechanoreceptor degradation

In our model, we assume that the stimulus is sensed by some number of mechanoreceptors in the cell membrane that are linked to ion channels, which open with a probability that is a function of the stimulus magnitude. If enough receptor linked channels open so that the change in voltage crosses a threshold, then an action potential fires. Meanwhile, every receptor that is open has a defined probability of being tagged for degradation (for example by phosphorylation). We assume that receptors are continuously synthesized at a constant rate, that receptors are degraded at a constant rate due to normal protein turnover, and that receptors that have become marked for degradation can also be degraded by an alternative degradation pathway that has a different rate than normal turnover.

We note that while this model is based on known biochemical functions that are widespread in cell biology (receptor inactivation, membrane potential, thresholded action potentials), it is still a highly simplistic model that leaves out many biochemical and molecular details. Model parameters are not based on direct experimental information from *Stentor* cells, for which such information is currently lacking. As such, the results of this model are not intended to be directly compared with numerical results from experiments. Instead, our goal is only to ask whether the model demonstrates key qualitative features of *Stentor* habituation that can be observed in experiments. With that in mind, we present the individual components of the model, each focused on a different biochemical process:

Modeling channel protein dynamics

The number of unmarked and marked receptors, as a function of time, are denoted U(t) and M(t). We represent the change in these two receptor pools by the following equations, where kdeg describes normal protein degradation and kdes describes active destruction of marked receptors.

$$\frac{dU}{dt} = k_{synth} - k_{deg}U \tag{1}$$

$$\frac{dM}{dt} = -\left(k_{deg} + k_{des}\right)M \tag{2}$$

Modeling mechanoreceptor opening

We represent the stimulus input as a series of delta functions of amplitude F, and assess channel opening only at those timepoints at which one of the stimuli in the series are being delivered. Given a stimulus F, we describe the probability of a mechanoreceptor channel opening by the following equation:

$$P_{open} = \frac{P_{max}}{1+e^{-Scale_F(F-F_{mid})}} \tag{3}$$

Where Fmid is an inflection point in the input-output curve.

Given Popen and the total number of receptors U(t)+M(t), we calculate the actual number of receptors that open in response to a given stimulus, Nopen, using Poisson statistics with parameter Popen*[U(t)+M(t)]

Membrane electrical model

Once the number of open channels is determined, we next calculate the effect on membrane potential. We model the membrane as a current source (reflecting ion pumps) in series with a resistor which incorporates the basal membrane resistance combined with any open membrane channels. With no receptor channels open, we assume some membrane conductance Sa. Given the membrane current source I, the basal membrane voltage, which we denote Vi, is given by

V1 = I/Sa (4)

During a stimulus, some number n=Nopen channels open, each with its own conductance Sb. The net conductance of the membrane thus changes to Sa + nSb. Now, the overall membrane voltage will become

V2 = I/(Sa + nSb) (5)

We model the action potential as occurring when the change in membrane voltage ΔV exceeds some threshold V_{thresh}. We calculate ΔV as follows

$$\Delta V = V_1 - V_2 = I\left(\frac{1}{S_a} - \frac{1}{S_a+nS_b}\right) = I\,\frac{S_a+nS_b-S_a}{S_a(S_a+nS_b)} = V_1\,\frac{nS_b}{S_a+nS_b} \quad (6)$$

Because both V1 and Sb are unknown parameters, we introduce the parameter Vi = V1Sb which yields the form of the equation used within the simulation program. When Sa >> nSb, the change in membrane voltage is approximately proportional to the number of open channels.

Modeling channel marking for degradation

After channels open, marking of channels for inactivation then takes place with a probability Ptag, with Ptag*U(t) determining the number of newly marked channels, which is added to M(t) and subtracted from U(t). These marked channels are then removed from the population according to the dynamics described above under Modeling Receptor Protein Dynamics.

Stochastic simulation

Using the equations above, we simulate the system using the Euler method with a time step of 0.01. We find a small (less than 10%) discrepancy in the response probabilities between the

stochastic and deterministic versions of the model, which is attributable to quantization effects on the receptor number when the average number is small.

Deterministic approximation

The stochastic model presented above is slow to run, making it difficult to explore various combinations of parameters and input sequences. We therefore developed a deterministic approximation in which we represent U and M by real numbers.

First, we calculate initial number of receptors by assuming a steady state condition in the absence of any stimuli, such that all receptors are unmarked, and the number of receptors is just ksynth/kdeg by solving equation 1 for steady state. Next, we calculate the probability of any given receptor becoming activated (open) using equation 3. Among the newly activated receptors a fraction is marked based on the parameter p_tag. The values of marked and unmarked receptors are then updated. Next, the minimum number of receptors that would need to be open in order to cross the activation threshold is calculated by solving equation 6 for n. Using the Poisson CDF, we then calculate the probability that enough receptors are activated, given the total number and probability of each receptor being open, to equal or exceed this minimal number. This value gives us the response probability which is the output of the model. Finally, we integrate equations 1 and 2 to determine the values of U and M at the timepoint when the next stimulus will arrive. The whole procedure is then repeated using these updated values, and this process is repeated for every timepoint. To simulate the forgetting phase after cessation of stimuli, a series of virtual stimuli are modeled such that at each virtual stimulus timepoint, the response probability is calculated as above, but the activation status of channels is not changed, such that U and M are allowed to evolve according to equations 1 and 2 with no effect from the virtual stimuli.

Parameter Sweep

The receptor inactivation model has a large number of parameters, for which experimental values are not yet available. In order to ask whether the model can in principle explain observed behavior, we need a way to choose parameter combinations that produce qualitatively reasonable outputs from the model. It is not computational feasible to use the stochastic simulation for a brute-force evaluation of all possible parameter combinations. Even the deterministic model described above is slow enough that it would make parameter sweeping prohibitively slow. Instead, we have developed the following procedure for numerically estimating system output from any given combination of parameters without the need for any simulations. For each parameter combination tested, we calculate the initial response probability, the steady-state (habituated) response probability, the habituation timescale, and the response recovery timescale. These four values are then compared to the desired values, and the parameter combination that minimizes the sum of the errors in all four outputs is taken as the optimal combination. We recognize that other weightings could be used to emphasize particular aspects of the habituation process.

Estimating response to initial stimulus for parameter sweeping

We directly determine the number of receptors from equation 1 as in the deterministic model. Next we calculate the initial response probability (response to the first stimulus applied a cell that had not previously been exposed) by calculating the activation probability (p_activation) based on the stimulus magnitude according to equation 3, then multiply the activation probability by the initial number of receptors to obtain the average number of open (activated) receptors.

Next, we use the inverse Poisson CDF to determine the minimum number of active receptors that would be observed with a probability equal to the target initial response probability.

From that number, we calculate the activation threshold from equation 6, assuming that the number of receptors calculated from the Poisson inverse CDF are active. This calculation directly gives the action threshold parameter Vthresh, which therefore does not need to be swept. Given the action threshold, we then calculate the number of receptors that would need to be open to give exactly that membrane potential.

Estimating Steady-state response for parameter sweeping

Once we have determined the initial response probability, we next determine the steady state probability after an infinite number of stimuli. Since the stimulus strength is the same as for the initial stimulus, p-activation is the same. The parameter action_threshold is the same for the whole simulation, so it applies here as well. Based on the conductance equation, the action_threshold parameter determines the number nmin of receptors that need to be active to trigger a response. So, if we know how many receptors there are, and p_activation, we can determine the probability that nmin of them will be activated.

Representation of cell state

Although all we care about in terms of the probability of contraction is the total number of receptors, in order to calculate changes in receptor number over time we need to recognize that marked and unmarked receptors decay at different rates, hence it is more convenient to keep track of both separately, and then add them up when we need to determine contraction probabilities. We thus represent cell state with two variables the number of marked and unmarked receptors.

Determining steady-state contraction probability

The basic approach for determining the steady state contraction probability is to first determine the steady-state number of marked and unmarked receptors, based on the steady state condition for each number, and then use them to get the steady state total receptor number from which the response probability can be easily calculated.

We use the following notation:

M0 = number of marked receptors just after a stimulus has arrived

M_- = number of marked receptors just before a stimulus arrives

U0 = number of unmarked receptors just after a stimulus has arrived
U_- = number of unmarked receptors just before a stimulus arrives

So at the moment a stimulus arrives, there are M- and U- marked and unmarked receptors, and then the stimulus determines how many of them will become activated via the parameter p_activation according to equation 3. Any marked receptors that open will just stay marked, but any unmarked receptors that are activated will become marked.

Therefore:

$M0 = M_- + ptag*pactivation*U_-$ (7)
$U0 = U_- - ptag*pactivation*U_-$ (8)

Let ϕ represent ptag*pactivation, then

$M0 = M_- + \phi U_-$ (9)
$U0 = U_- - \phi U_- = (1-\phi)U_-$ (10)

Now, starting with M0 and U0, we let each evolve forward in time according to the differential equations

$$\frac{dU}{dt} = k_{synth} - k_{deg}U \quad (11)$$

$$\frac{dM}{dt} = -\left(k_{deg} + k_{des}\right)M \quad (12)$$

After a given interval τ between successive stimuli, we have

$$M(\tau) = M_0 e^{-\left(k_{deg}+k_{des}\right)\tau} \quad (13)$$

$$U(\tau) = \frac{k_{synth}}{k_{deg}} + \left(U_0 - \frac{k_{synth}}{k_{deg}}\right)e^{-k_{deg}\tau} \quad (14)$$

At steady state, M- = M(τ)=Mss and U- = U(τ)=Uss

Let θ=ksynth/kdeg

Then since the equation for U only depends on U, we can solve for Uss as follows:

$$Uss = \theta + (U_0 - \theta)e^{-k_{deg}\tau} \quad (15)$$

$$Uss = \theta + \left((1 - \emptyset)Uss - \theta\right)e^{-k_{deg}\tau} \quad (16)$$

$$Uss - (1-\emptyset)Usse^{-k_{deg}\tau} = \theta\left(1 - e^{-k_{deg}\tau}\right) \quad (17)$$

$$Uss\left[1 - (1-\emptyset)e^{-k_{deg}\tau}\right] = \theta\left(1 - e^{-k_{deg}\tau}\right) \quad (18)$$

Which gives the steady state number of unmarked receptors:

$$Uss = \frac{\theta\left(1 - e^{-k_{deg}\tau}\right)}{\left[1 - (1-\emptyset)e^{-k_{deg}\tau}\right]} \quad (19)$$

Now we can plug this into the equation for M as follows:

$$Mss = (Mss + \emptyset Uss)e^{-(k_{deg} + k_{des})\tau} \quad (20)$$

$$Mss\left[1 - e^{-(k_{deg} + k_{des})\tau}\right] = \emptyset Usse^{-(k_{deg} + k_{des})\tau} \quad (21)$$

Which gives the steady state number of marked receptors:

$$Mss = \frac{\emptyset Usse^{-(k_{deg} + k_{des})\tau}}{\left[1 - e^{-(k_{deg} + k_{des})\tau}\right]} \quad (22)$$

From equations 19 and 22, we obtain the total number of receptors at steady state, Nss = Mss + Uss, From which we can calculate the number that activate in response to the stimulus based on p_activation (which was determined by the stimulus strength). Finally, we use the Poisson CDF to determine the probability that, given this average number of activated receptors, a sufficient number (nmin, calculated as above) are activated to cross the action threshold. This yields the steady state contraction probability.

Estimating Learning timescale for parameter sweeping

Using the initial contraction probability and the steady state contraction probability that have been calculated, we determine the halfway point between the two probabilities. We now seek to determine what the receptor number would be to attain that halfway-point response probability. To do this, once n_min, the required number of receptors that need to open in order to cross the activation threshold, has been calculated, we generate a lookup table that contains the Poisson parameter necessary for a Poisson process such that the number of counts will exceed n_min as a function of the desired probability. The Poisson parameter will then equal n_receptor*prob_acdtivaiton, so given p_activation (which only depends on the stimulus magnitude and the parameters of equation 3), we can determine n_receptor at the

halfway response point. Next we calculate the time required to reach this point. Assuming exponential decay of the receptor number from its initial value, we calculate the remaining number of receptors after the first stimulus interval, i.e. the number that will be present at the start of the next stimulus. From this, we take the ratio ρ of receptor numbers after and before the first interval. Assuming exponential decay, this decay ratio should approximately hold for all intervals, and we use this to estimate the number of stimuli required to pass the halfway point.

Defining N_{init} as the initial receptor number prior to any stimuli, and N_H has the number of receptors at the half response point, the number of stimuli take to reach the half response will be

$$Steps = \frac{\ln N_H - \ln N_{init}}{ln\rho} \quad (23)$$

The learning half-time tlearn is thus given by:

Tlearn = Steps*stimulus_interval (24)

Estimating Forgetting timescale for parameter sweeping

To calculate the forgetting lifetime, we recognize that at the end of the last stimulus, period, the number of marked and unmarked receptors will be Mss and Uss. No more marking occurs during the forgetting period, since no stimuli are applied, thus each of these two quantities will undergo exponential decay with its own rate. The total number of receptors will thus decay with an overall decay rate given by the same formula used to calculate fluorescence lifetime of a mixture of two fluorophores (see Lakowicz eq 3.53).

Letting αm = Mss/(Mss+Uss) and αU = Uss/(Mss+Uss)

And defining the average receptor lifetimes

$$\tau_M = \frac{1}{k_{deg}+k_{des}} \quad (25)$$

And

$$\tau_U = \frac{1}{k_{deg}} \quad (26)$$

And using the formulate for average lifetime we get

$$\langle\tau\rangle = \frac{\alpha_M\tau_M^2+\alpha_U\tau_U^2}{\alpha_M\tau_M+\alpha_U\tau_U} \quad (27)$$

This is the decay time for the receptor number, and the reciprocal is the decay rate constant for receptor number, krecovery = 1/<t>.

With this decay rate in hand, we can calculate the time for the receptor number at steady state to increase to a number that will restore the response probability to halfway between steady state and initial response probability (which is the same number of receptors as calculated above for the learning rate)

$$\tau_{forget} = \frac{ln\left(\frac{(N_H - N_{init})}{(N_{ss} - N_{init})}\right)}{-k_{recovery}} \tag{28}$$

Parameter search procedure

For the simulation results in this paper, we carried out the parameter procedure with target values given in Table 1.

Table 1. Target output values for parameter sweep

value	Low force	High force	High frequency
Initial response	0.8	0.9	0.8
Habituated response	0.3	0.85	0.3
Learning timescale	2	12	0.5
Forgetting timescale	3	12	3

Using the above procedure, we scanned the following parameters over the following ranges:
Ksynth 4.0 - 8.0 in steps of 0.5
P_degradation 0.01 - 0.2 in steps of 0.01
Io_function_midpoint 0 - 0.01 in steps of 0.00005
Io_function_scale 0.05 - 1.0 in steps of 0.05
Conductance b 0.00005 - 0.005 in steps of 0.00005
P_tag 0 - 0.3 in steps of 0.05
P_destruction 0.3 - 0.5 in steps of 0.05

These ranges were determined by adjustment using iterative runs of the simulation under different ranges until the procedure found values that were not at either end of their range for any parameter.

Three model parameters did not need to be swept since they only occur in combination with other parameters that were being swept:
Vi was set to 1 such that action_threshold was interpreted as a fraction of Vi.
Io_function_max was set to 1 since the other values can be rescaled accordingly.

Conductance_a was set to 1000 but conductance b can be rescaled for any other value of conductance a.

The result of this parameter sweep process yielded the following model parameters that were used for all simulations shown in this paper:
rate_synthesis 7
p_degradation 0.2
io_function_midpoint 0.01
io_function_scale 0.45
conductance_ b0.00025
p_tag 0.1
p_destruction 0.45
action_threshold 0.017

We note that this parameter search was not an attempt to determine actual parameter values by fitting, but merely an effort to show that the model can, in principle, produce similar behavior to actual cells. We make no claims with respect to uniqueness or optimality of this parameter set - our results do not by any means preclude other parameter combinations giving equal or better performance.

Experimental methods for testing model predictions using Stentor cells

Stentor coeruleus cells, originally obtained from VWR (Ward's Science 470176-586; Radnor, PA), were grown using a modified version of a previously described culturing protocol (Lin 2018). Cells were grown in a 946-mL glass bowl (Pyrex 1075428; Downers Grove, IL) filled halfway with pasteurized spring water (Carolina Biological 132458; Burlington, NC). Each culture was started with approximately 200-500 cells transferred into a new bowl with fresh media. When not in use, *Stentor* cultures were stored in a dark drawer at room temperature. Cells used for habituation experiments came from cultures that were 2.5-6 weeks old. To the extent possible, cells for habituation experiments were chosen such that they had a healthy trumpet shape when fully extended (**Figure 1B**) and did not show any preliminary signs of entering mitosis. For any given set of experimental comparisons, cells from both the experimental and control groups were sourced from the same culture. The rate sensitivity experiments, however, were an exception in that the final replicate of the group of cells trained with a frequency of 1 tap per 1.2 seconds was sourced from a different culture due to contamination of the original culture.

Solid cultures of *Chlamydomonas reinhardtii*, grown on Tris-Acetate-Phosphate (TAP) agar plates under bright light, were used as the food source for *Stentor* cultures. Sterile inoculating loops (BD Difco 220217; Franklin Lakes, NJ) were used to scrape approximately 9-15 mg of solid *Chlamydomonas* culture from a TAP plate. The *Chlamydomonas* bolus was dislodged into the *Stentor* culture through manual stirring and shaking of the sterile loop. The bolus was dispersed in the culture by gently pipetting up and down with a P1000 pipette. Remaining large, insoluble fragments of the *Chlamydomonas* bolus were subsequently removed from the *Stentor* culture using the same P1000 pipette. Media removed during this cleaning process was

replenished with fresh pasteurized spring water. When experiments were underway, *Stentor* were fed approximately every 1-2 days, depending on culture density. Prior to any experiments on a given day, *Stentor* were examined under dark field illumination to confirm the presence of *Chlamydomonas* inside *Stentor* food vacuoles, thus ensuring that the *Stentor* cells were consistently well fed prior to experimentation.

Stentor habituation experiments were carried out at room temperature using the protocol described in Rajan et al. 2023b. Following an acclimation period of approximately two hours, mechanical taps were delivered to the cells at a specified force and frequency using an Arduino-controlled habituation device. *Stentor* behavior over the course of the habituation experiments was recorded on a USB microscope (Celestron 44308; Torrance, CA) and the fraction of cells contracted at various time points during training was subsequently quantified.

For experiments testing the ability of *Stentor* to habituate to low-force stimuli while experiencing high-force stimuli, the cells were given 19 level 3 or level 2 (high-force) stimuli and subsequently given 41 level 4 (low-force) stimuli, all at a frequency of 1 stimulus per minute. Force levels are defined in Rajan et al. 2023b. To assess the effects of interleaving high-force and low-force stimuli, the cells were given one tap per minute alternating between level 4 taps and level 3 taps. Cells in the control groups received one level 4 tap per minute.

To test rate sensitivity, cells were trained with level 4 stimuli for 12 hours and then tested for memory retention following cessation of training. One group of cells was trained at a frequency of 1 tap per min while the other was trained at a frequency of 1 tap per 1.2 seconds. Forgetting was tested by delivering level 4 taps at 1.5, 5, 10, 20, 30, 60, and 90 minutes post-training and then quantifying the fraction of cells contracted at each time point.

Acknowledgments
We acknowledge stimulating discussions with students in UCSF Cellular Cognition course held 2012 - 2016 during our initial efforts to reproduce *Stentor* habituation and study its properties in the lab, as well as with students and faculty in the Physiology Course at the Marine Biological Laboratory in Woods Hole where we continued to develop experiments on *Stentor* learning. We also thank current and former members of the Marshall lab, particularly Mark Slabodnick and Tatyana Makushok, as well as Adam Frost, and Steve Beckwith for discussions about this project. This work was supported by NSF grant MCB-2012647 and NIH grant R35 GM130327.

Figure Legends

Figure 1. Habituation in the single-celled organism *Stentor coeruleus*. (**A**) When not disturbed, a *Stentor* cell extends into a cone shape, attached at its base to a leaf or other surface by means of a holdfast, and allowing it to draw in food using flow generated by a ring of cilia at the anterior end. When a *Stentor* cell experiences a mechanical stimulation, such as from a predator, it contracts by means of myonemes, which consist of long bundles of contractile EF hand proteins (shown in red). (**B**) Images of a cluster of *Stentor* cells in the extended and contracted states. (**C**) Habituation in S*tentor*: following repeated stimulation at a constant force, a population of cells gradually becomes less likely to contract in response to further stimulation. The rate and extent of habituation is less when cells are stimulated with larger magnitude force. (**D**) Habituation is step-like in individual cells. Red arrows indicate contraction events, showing that a cell typically starts out responding to every stimulus, but then appears to switch to a much lower rate of contraction. (**E**) A previously described two-state model (Rajan 2023a) suggested by the switch-like behavior of individual cells. The model represents a cell as being in two possible states, a responsive state which contracts to a stimulus with a probability P1, and a non-responsive state which contracts with probability P2. Each time a stimulus is applied, the cell can switch between the two states with probability p12 of going from the response to the nonresponsive state, and probability p21 of going from the nonresponsive back to the responsive state.

Figure 2. Biochemical model for habituation in *Stentor* based on activity-dependent receptor inactivation. (**A**) Diagram of model showing mechanoreceptors at the cell surface modeled as ion channels fluctuating between open and closed states. While in the open state, the receptor/channel can be internalized and marked for degradation. Ion flow through the channels alters the membrane potential, which can trigger opening of a voltage dependent calcium channel. Influx of calcium leads to cell contraction. (**B**) Simulation of deterministic model for *Stentor* habituation. (blue) total receptor number, normalized to maximum value. (green) number of receptors marked for degradation/inactivation, normalized to maximum total receptor number. (red) probability of contraction. This simulation modeled a series of 30 stimuli applied at a frequency of 1 per minute. The reduced probability of contraction with successive stimuli indicates habituation. After 30 stimuli, the stimulus ceased and the probability of contracting if a stimulus were to be applied was then calculated for 30 more intervals, to quantify the response recovery. Return of the contraction probability to its initial value indicates recovery of response (forgetting). In this simulation, both habituation and response recovery occur on a timescale comparable to what has been reported in actual cells. (**C**) Lack of dishabituation in the receptor inactivation model. In this simulation, using the same parameters as panel B, 30 stimuli were applied to achieve habituation, followed by a single stimulus ten times greater, which caused a close to 100% contraction probability. After the single strong impulse, 30 more normal force stimuli were applied, and the response probability immediately shifted back to its previous habituated level, indicating that the model does not

show dishabituation or sensitization. **(D)**. Example result of a stochastic simulation of receptor inactivation model. (blue) total receptor number, (orange) number of marked receptors, (purple) contraction events. In this simulation, stimuli were applied at a frequency of one per minute, and the simulation timestep was 0.01 minutes. Note that receptors can become marked for inactivation every time a stimulus is applied, regardless of whether the cell contracts, which is why the orange curve sometimes fluctuates upwards in between contractions. (**E**) Habituation in the stochastic implementation of the receptor inactivation model. Plot shows response probability averaged over 400 simulations confirming that habituation similar to that seen in actual cells occurs in the stochastic version of the model using the same parameters as panel D. (**F**) Statistical test for switch-like behavior in the stochastic model. Beeswarm plot shows p values for test for one and for two steps, indicating that a majority of cells show a single step-like response.

Figure 3. Predicted effect of stimulus magnitude and frequency on habituation. (**A,B**) Simulations of two different force stimuli with the stimulus in panel B tenfold higher (10 force units) than that in panel A (1 force unit). With the high force stimulus, receptor number still decrease (blue curve) but this does not lead to a large drop in response probability because the large force is able to trigger a larger fraction of the remaining receptors. (**C**) Response curves for different stimulus forces, showing that habituation is faster and more extensive for smaller forces, and slower and less extensive for larger forces. (**D**) Simulation using the same stimulus magnitude as panel A, but with a ten-fold higher frequency. Comparing panels A and D it is apparent that the rate of habituation is greatly increased with this high frequency stimulus. (**E**) Response probability at the end of the stimulus sequence versus the inter-stimulus interval (τ) of the stimulus sequence. In all case, the same total number of stimuli were applied.

Figure 4. Habituation of low-force response during high-force stimulation: simulations and experiments. (**A**) simulation showing that a series of high-magnitude stimuli that cause little observable habituation to the high force stimulus lead to a decreased response to a lower force stimulus. Blue markers show that receptor number drops during the high force stimulus part of the sequence, which explains why the response to the subsequent low force stimuli starts out at a low level. (**B**) Simulation using just the low force stimulus from panel A included for comparison. (**C**) Experimental measurement based on the simulation of panel A. In this experiment, a sequence of 19 high force taps (red squares; Force level 3; N=59-85) was applied at a rate of 1 tap per minute, after which 41 low force (force level 4) taps were applied at 1 tap per minute. Despite the fact that that the cells had never experienced a low force tap, but only high force taps to which they do not significantly habituation, they indeed showed a reduced probability of response to the low force tap, comparable to what is seen if the same experiment had been carried out using only low force taps (black circles; force level 4, N=51-87). A similar effect is seen when an even higher force is used for the first 19 taps followed by the same low force (level 3) for the remaining 41 taps (green triangles; N=70-84). Error bars signify standard error. (**D**) Simulation of interleaved high and low force stimuli, showing that the response to the low force stimulus undergoes habituation but does not cause habituation for the large force stimulus. Blue markers show that receptor number drops after both types of stimuli. (**E**) Experimental measurement of interleaved high (red squares; force level 3; N=62-77) and low

(red circles; force level 4; N=59-71) magnitude stimuli applied at an n overall rate of one stimulus per minute, with the high force taps alternating with the low force taps. Black triangles indicate a control experiment using only the lower force level taps with identical timing (force level 4; N=51-60). Error bars signify standard error calculated from binomial statistics. As predicted by the model, the response to the low force stimuli shows extensive habituation even though the response to the alternating high force stimuli does not.

Figure 5. Stimulus frequency does not affect response recovery time: simulations and experiments. (**A,B,C**) Three simulations using the same model parameters and stimulus magnitude but different stimulus periodicities (A 1 minute, B 0.25 minutes, C 0.1 minutes). After the stimulus ends, the response recovery can be seen to occur at a similar timescale in the first two cases. With the extremely high frequency stimulation in panel C, response recovery takes longer than for the lower frequency stimuli. (**D**) Response recovery time versus stimulus frequency. For each simulation used to generate this curve, habituation was carried out until the response probability reached a steady state. Recovery time is defined here as the time for the response probability to recover halfway between the probabilities seen in fully habituated and fully naive cells. (**E**) Experimental measurement of response recovery following complete habituation to two stimuli applied at frequencies of 1 tap per minute (red squares) or 1 tap per 1.2 seconds (blue circles), showing that the response recovery is virtually the same in both cases. Error bars signify standard error of the mean.

Supplementary Figure S1. Bode plot of frequency response of the receptor inactivation model. Amplitude gain is calculated from the probability of response data in **Figure 3E**, with each value normalized by the maximum value of 0.8 which we take as indicating full signal transmission. Frequency is in units of log10 of inverse minutes.

References

Byrne JH. 1982. Analysis of synaptic depression contributing to habituation of gill-withdrawal reflex in Aplysia californica. *J. Neurophysiol*. 48, 431-438

Davis M. 1970. Effects of interstimulus interval length and variability on startle-response habituation in the rat. *J. Comparative Physiol. Psychology* 72, 177-192

Baluska F, Levin M. 2016. On Having No Head: Cognition throughout Biological Systems. *Front Psychol. 7*, 902.

Bray D. 2011. *Wetware: A computer inside every living cell*. Yale University Press, 280 pp.

Condon A, Kirchner H, Lariviere D, Marshall WF, Noireaux V, Tlusty T, Fourmentin E 2018. Will biologists become computer scientists? EMBO Reports pii: e46628

Dexter JP, Prabakaran S, Gunawardena J. 2019. A Complex Hierarchy of Avoidance Behaviors in a Single-Cell Eukaryote. *Curr. Biol*. *29*, 4323-4329.e2

Estadella I, Pedrós-Gámez O, Colomer-Molera M, Bosch M, Sorkin A, Felipe A. 2020. Endocytosis: A Turnover Mechanism Controlling Ion Channel Function. *Cells*. 9, 1833

Gershman SJ. 2024. Habituation as optimal filtering. *iScience* 27, 110523

Groves PM, Thompson RF. 1970. Habituation: A dual-process theory. *Psychological Review*, 77, 419–450.

Harris JD. 1943. Habituatory response decrement in the intact organism. *Psychological Bulletin*. 40, 385-422.

Huang B, Pitelka DR. 1973. The contractile process in the ciliate, Stentor coeruleus. I. The role of microtubules and filaments. *J. Cell Biol*. 57, 704-28.

Jennings, H.S. 1902. Studies on reactions to stimuli in unicellular organisms. IX. On the behavior of fixed infusoria (Stentor and Vorticella) with special reference to the modifiability of protozoan reactions. *Am. J. Physiol*. 8, 23-60.

Jennings HS. 1906. *Behavior of the Lower Organisms*. Columbia University Press, New York, NY, USA.

Jones AR, Jahn TL, Fonseca JR. 1970. Contraction of protoplasm. III. Cinematographic analysis of the contraction of some heterotrichs. *Journal of Cellular Physio*logy. 75, 1-7.

Katta S, Krieg M, Goodman MB. 2015. Feeling force: physical and physiological principles enabling sensory mechanotransduction. *Ann. Rev. Cell Mol. Biol*. 31, 347-71.

Kholodenko BN. 2003. Four-dimensional organization of protein kinase signaling cascades: the roles of diffusion, endocytosis and molecular motors. *J Exp Biol*. 206, 2073–2082.

Kuenen LPS, Baker TC. 1981. Habituation versus sensory adaptation as the cause of reduced attraction following pulsed and constant sex pheromone pre-exposure. *J. Insect Physiol*. 27, 721-726.

Lakowicz JR. 1983. *Principles of fluorescence spectroscopy*. Plenum Press, NY. 496 pp.

Larson BT. 2023. Perspectives on Principles of Cellular Behavior from the Biophysics of Protists. *Integr Comp Biol*. 63, 1405-1421

Lin AW, Man H. 2013. Ubiquitination of Neurotransmitter Receptors and Postsynaptic Scaffolding Proteins. *Neural Plast*. 432057.

Lin A, Makushok T, Diaz U, Marshall WF. 2018. Methods for the Study of Regeneration in Stentor coeruleus. *J. Vis. Exp (JoVE).* 136, 57759

Lin A, Piehowski PD, Tsai CF, Makushok T, Yi L, Diaz U, Yan C, Summers D, Sood P, Smith RD, Liu T, Marshall WF. 2022. Determining protein polarization proteome-wide using physical dissection of individual Stentor cells. *Curr. Biol*. 32, 2300-2308

Maloney M, McDaniel W, Locknar S, Torlina H. 2005. Identification and localization of a protein immunologically related to caltractin (centrin) in the myonemes and membranelles of the heterotrich ciliate Stentor coeruleus. *Journal of Eukaryotic Microbiology*, 52, 328-338.

Marshall WF. 2019. Cellular Cognition: Sequential Logic in a Giant Protist. *Curr Biol*. 29, R1303-R1305

Marshall WF. 2021. Regeneration in Stentor coeruleus. *Front. Cell Dev. Biol*. 9, 753625

Newman E. 1972. Contraction in Stentor coeruleus: a cinematic analysis. *Science* 177, 447-449.

Phillips R. 2020. *The molecular switch: Signaling and Allostery*. Princeton University Press.

Rajan D, Makushok T, Kalish A, Acuna L, Bonville A, Correa Almanza K, Garibay B, Tang E, Voss M, Lin A, Barlow K, Harrigan P, Slabodnick MM, Marshall WF. 2023a. Single-cell analysis of habituation in Stentor coeruleus. *Current Biology*. 33, 241-251

Rajan D, Chudinov P, Marshall W. 2023b. Studying Habituation in Stentor coeruleus. *J Vis Exp*. 191, 10.3791/64692

Rankin CH, Abrams T, Barry RJ, Bhatnagar S, Clayton DF, Colombo J, Coppola G, Geyer MA, Glanzman DL, Marsland S, McSweeney FK, Wilson DA, Wu CF, Thompson RF. 2009. Habituation revisited: an updated and revised description of the behavioral characteristics of habituation. *Neurobiol Learn Mem*. 92, 135-8

Rankin CH, Broster BS. 1992. Factors affecting habituation and recovery from habituation in the nematode Caenorhabditis elegans. *Behavioral Neurosci*. 106, 239-242

Rosendale M, Jullie D, Choquet D, Perrais D. 2017. Spatial and Temporal Regulation of Receptor Endocytosis in Neuronal Dendrites Revealed by Imaging of Single Vesicle Formation. *Cell Reports* 18, 1840-1847.

Shankaran H, Wiley HS, Resat H. 2007. Receptor downregulation and desensitization enhance the information processing ability of signalling receptors. *BMC Syst Biol* 1, 48.

Slabodnick MM, Ruby JG, Dunn JG, Feldman JL, DeRisi JL, Marshall WF. 2014. The kinase regulator mob1 acts as a patterning protein for Stentor morphogenesis. *PLoS Biol*. 12, e1001861;

Slabodnick MM, Ruby JG, Reiff SB, Swart EC, Gosai S, Prabakaran S, Witkowska E, Larue GE, Fisher S, Freeman RM, Gunawardena J, Chu W, Stover NA, Gregory BD, Nowacki M, Derisi J, Roy SW, Marshall WF, Sood P. 2017. The macronuclear genome of Stentor coeruleus reveals tiny introns in a giant cell. *Curr. Biol*. 27, 569-75.

Sood P, Lin A, Yan C, McGillivary R, Diaz U, Makushok T, Nadkarni AV, Tang SKY, Marshall WF. 2022. Modular, cascade-like transcriptional program of regeneration in Stentor. *Elife* 11, e80778.

Staddon JER. 1993. On rate-sensitive habituation. *Adaptive Behavior* 1, 421-436.

Staddon JER, Higa JJ. 1996. Multiple time scales in simple habituation. *Psychol. Rev.,* 103, 720–33

Tang SKY, Marshall WF. 2018. Cell Learning. *Curr. Biol*. *28*, R1180-1184

Tartar V. 1961. *The Biology of Stentor*. Pergammon Press.

Thompson RF, Spencer WA. 1966. Habituation: a model phenomenon for the study of neuronal substrates of behavior. *Psych. Rev.* *73*, 16-43.

Torre V, Ashmore JF, Lamb TD, Menini A. 1995. Transduction and Adaptation in Sensory Receptors. *J Neuroscience*. 15, 7757-7768.

Trinh MK, Wayland MT, Prabakaran S. 2019. Behavioral analysis of single-cell aneural ciliate, Stentor roeseli, using machine learning approaches. *J. R. Soc. Interface* 16, 20190410.

Vertosick FT. 2002. *The Genius Within: Discovering the Intelligence of Every Living Thing*. Harcourt, 368 pp.

Wood DC. 1970a. Parametric studies of the response decrement produced by mechanical stimuli in the protozoan, Stentor coeruleus. *J Neurobiol.* 1, 345-360.

Wood DC. 1970b. Electrophysiological correlates of the response decrement produced by mechanical stimuli in the protozoan, Stentor coeruleus. *J. Neurobiol*. 2, 1-11.

Wood, D.C. 1972. Generalization of habituation bewteen different receptor surfaces of Stentor. *Physiol. Behavior* 9, 161-165.

Wood DC. 1988a. Habituation in Stentor: a response-dependent process. *J Neurosci*. 8, 2248-2253.

Wood DC. 1988b. Habituation in Stentor: produced by mechanoreceptor channel modification. *J Neurosci*. 8, 2254-2258.

Wood, D. C. 1989. Localization of mechanoreceptors in the protozoan, Stentor coeruleus. *J Comp Physiol A.* 165, 229-235.

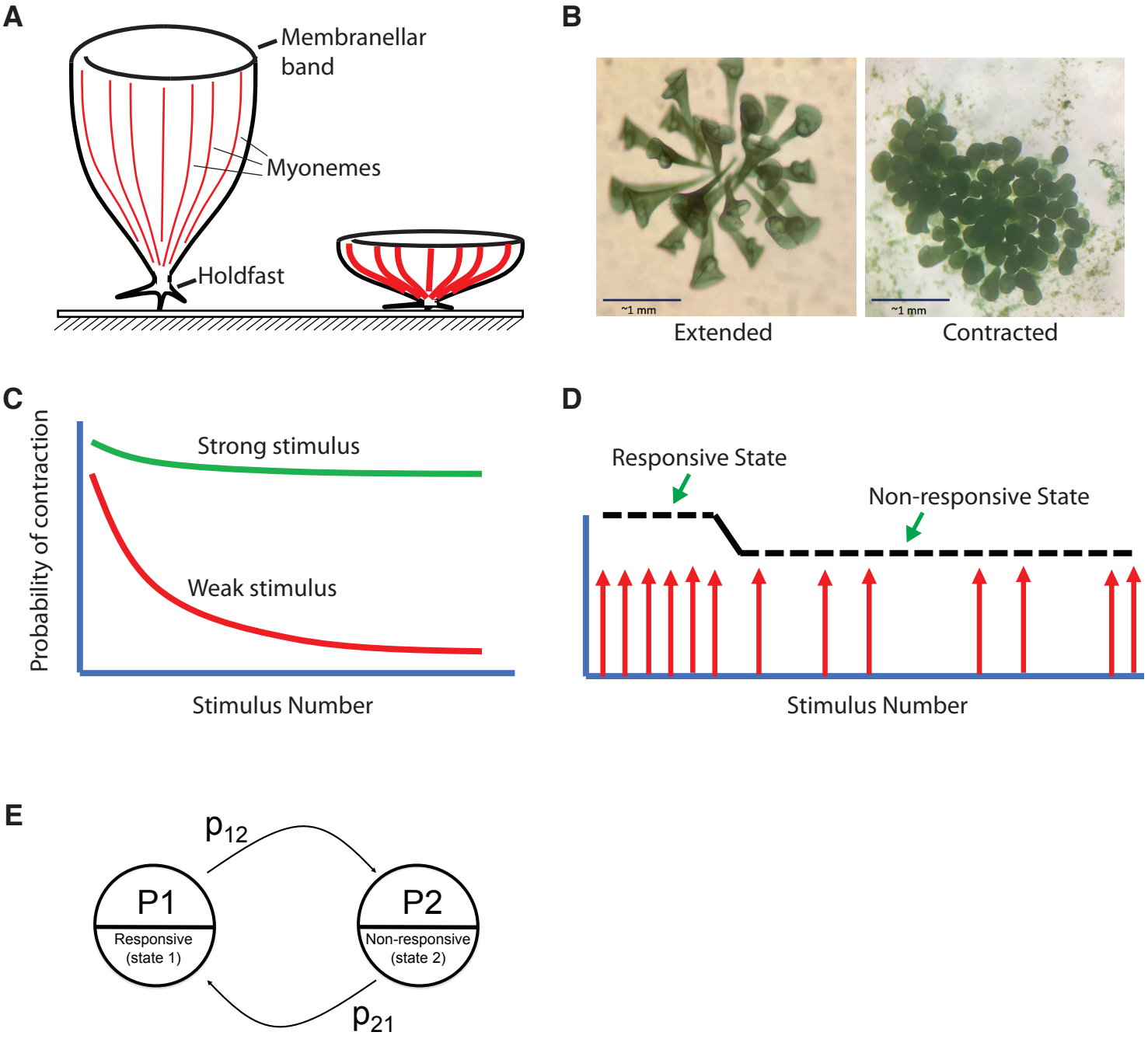
A
Membranellar band
Myonemes
Holdfast
B
~1 mm
~1 mm
Extended
Contracted
C
Probability of contraction
Strong stimulus
Weak stimulus
Stimulus Number
D
Responsive State
Non-responsive State
Stimulus Number
E
p12
P1
Responsive (state 1)
P2
Non-responsive (state 2)
p21

Figure 1

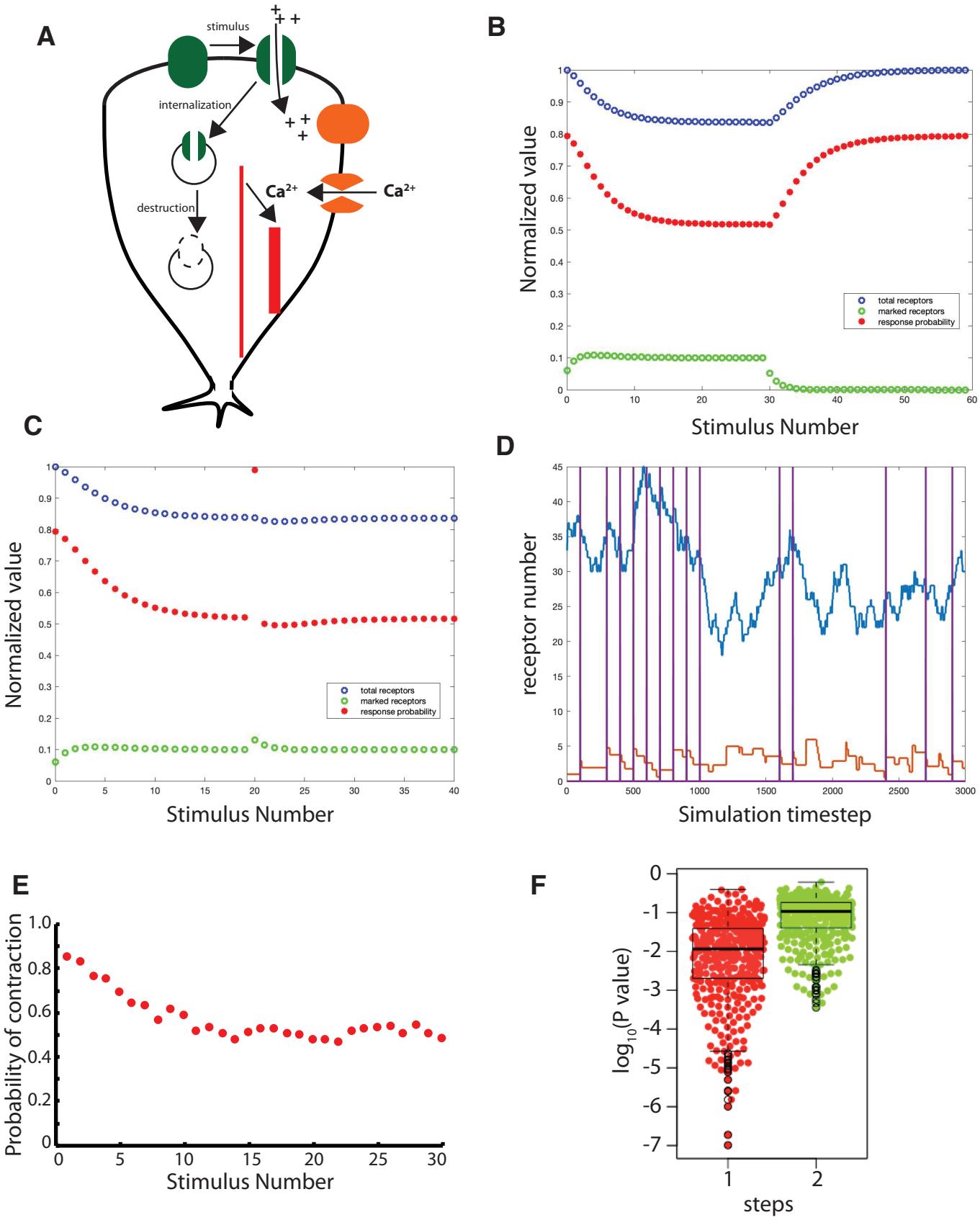
A
stimulus
internalization
destruction
Ca2+
Ca2+
B
Normalized value
Stimulus Number
total receptors
marked receptors
response probability
C
Normalized value
Stimulus Number
total receptors
marked receptors
response probability
D
receptor number
Simulation timestep
E
Probability of contraction
Stimulus Number
F
log10(P value)
steps

Figure 2

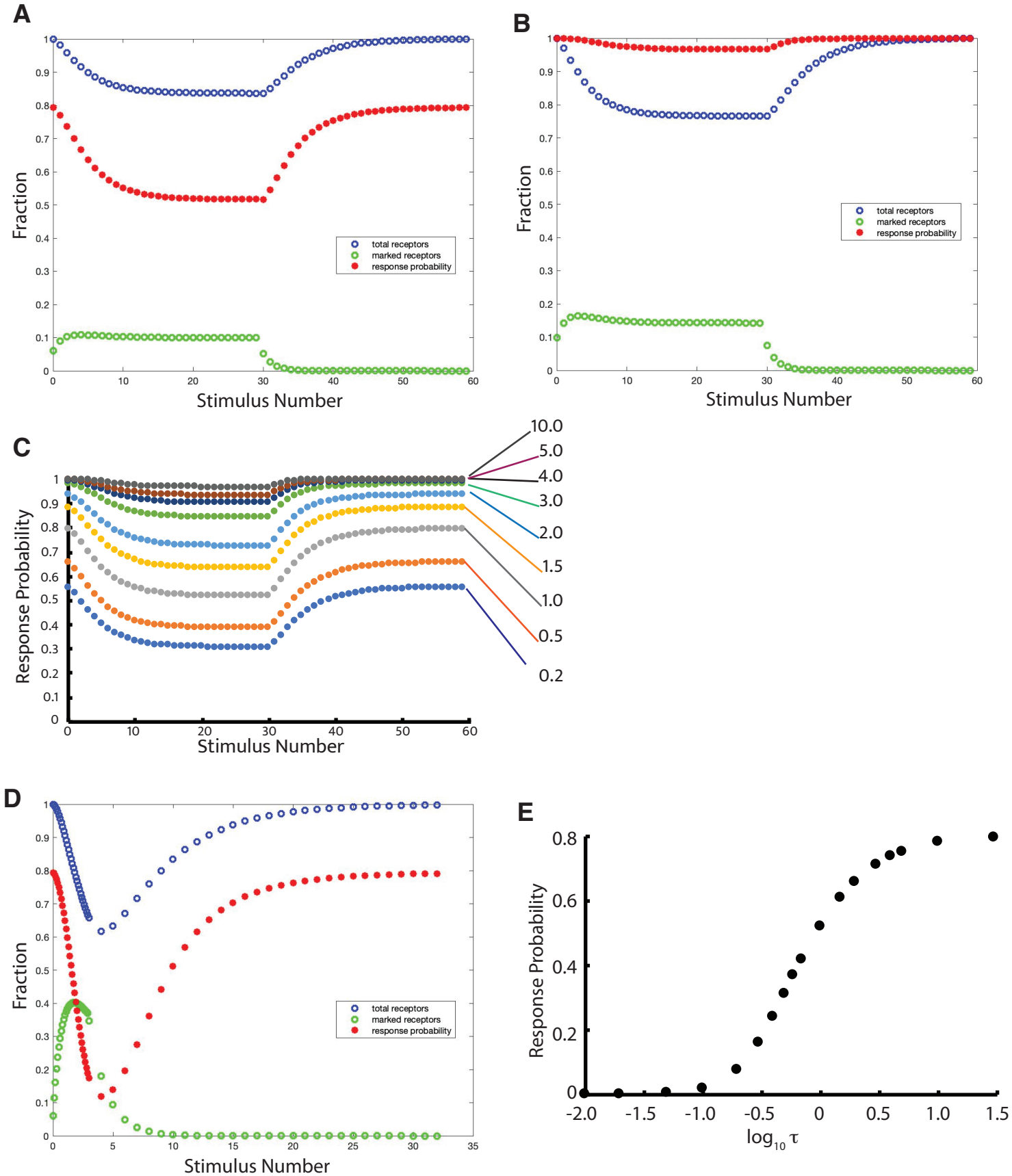
A
Fraction
Stimulus Number
total receptors
marked receptors
response probability
B
Fraction
Stimulus Number
total receptors
marked receptors
response probability
C
Response Probability
Stimulus Number
10.0
5.0
4.0
3.0
2.0
1.5
1.0
0.5
0.2
D
Fraction
Stimulus Number
total receptors
marked receptors
response probability
E
Response Probability
log10 τ

Figure 3

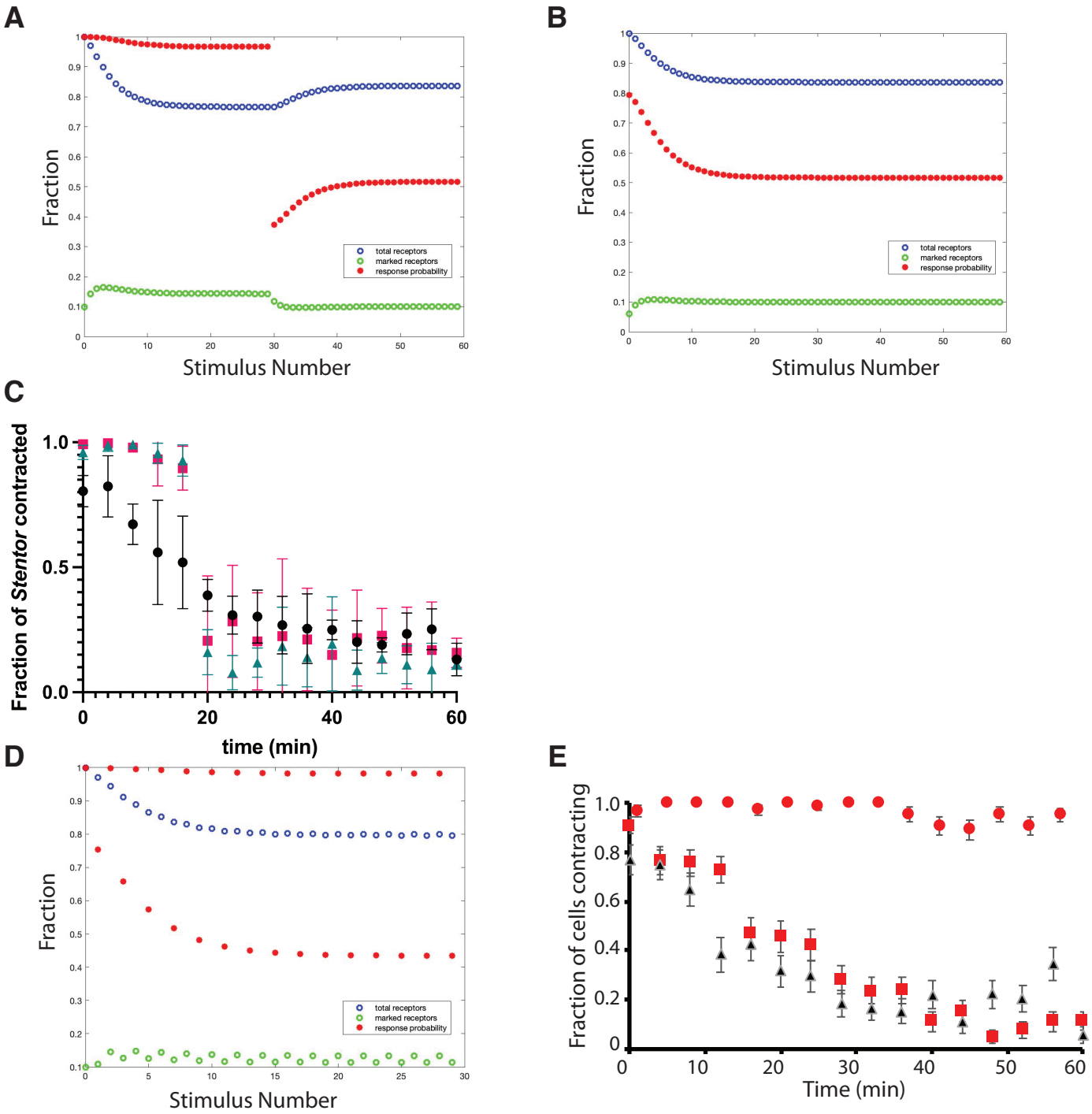
A
Fraction
Stimulus Number
total receptors
marked receptors
response probability
B
Fraction
Stimulus Number
total receptors
marked receptors
response probability
C
Fraction of Stentor contracted
time (min)
D
Fraction
Stimulus Number
total receptors
marked receptors
response probability
E
Fraction of cells contracting
Time (min)

Figure 4

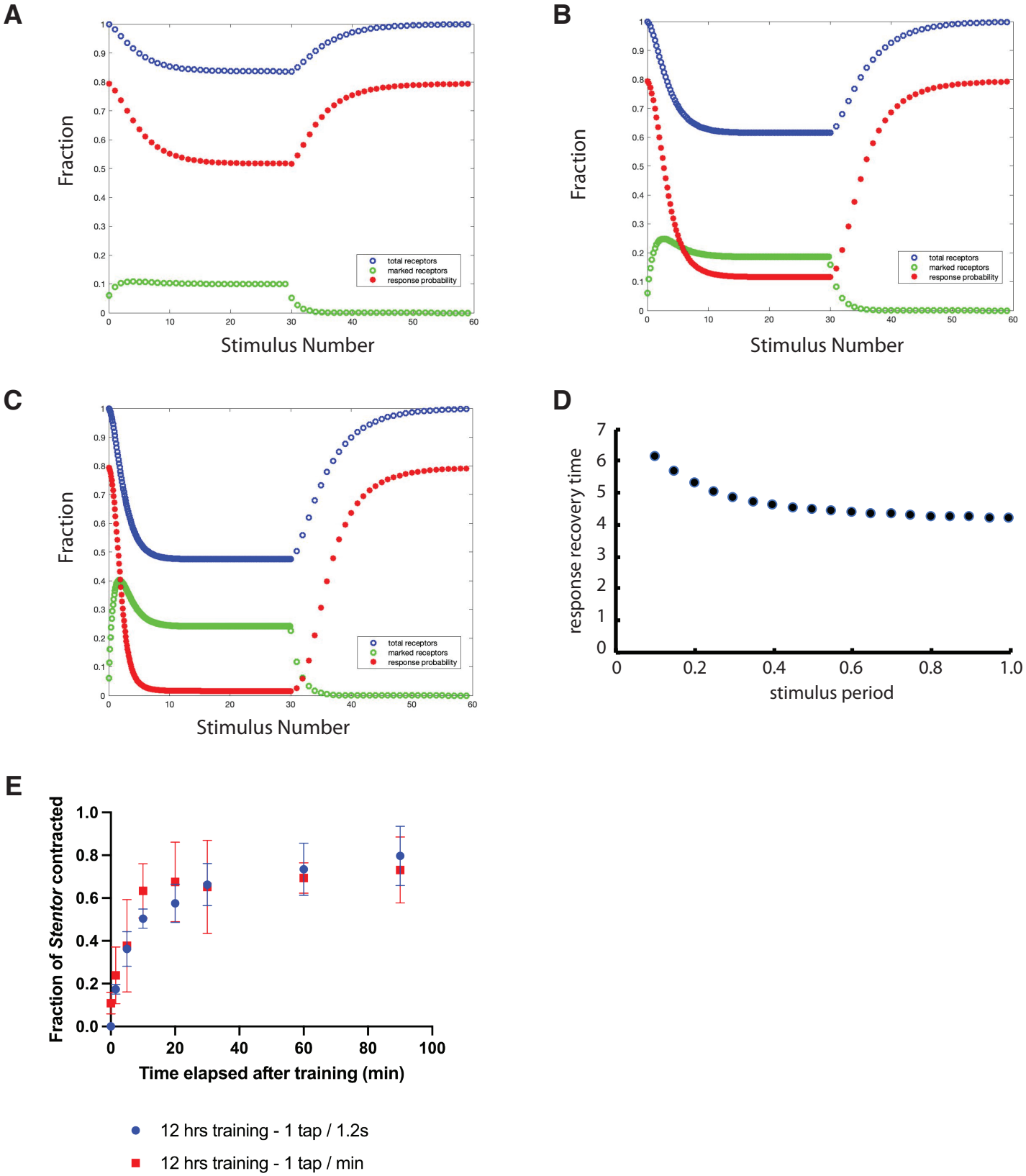
A
Fraction
Stimulus Number
total receptors
marked receptors
response probability
B
Fraction
Stimulus Number
total receptors
marked receptors
response probability
C
Fraction
Stimulus Number
total receptors
marked receptors
response probability
D
response recovery time
stimulus period
E
Fraction of Stentor contracted
Time elapsed after training (min)
12 hrs training - 1 tap / 1.2s
12 hrs training - 1 tap / min

Figure 5

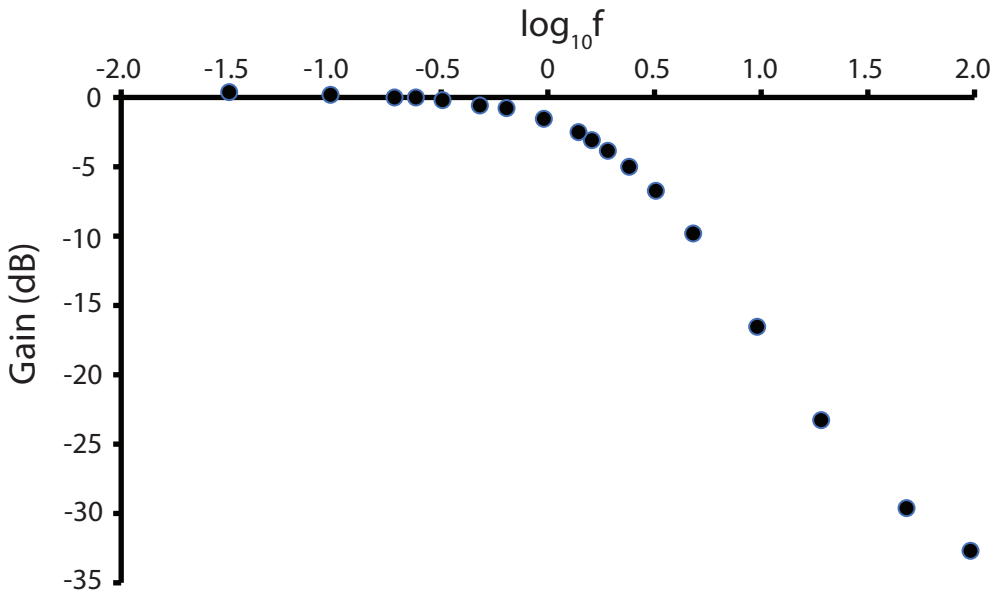

Figure S1